Chemical Engineering Journal 154 (2009) 34–44

Contents lists available at ScienceDirect

Chemical Engineering Journal

journal homepage: www.elsevier.com/locate/cej

Kinetics of the biofuels-assisted SCR of NO_x over Ag/alumina-coated microchannels

J.R. Hernández Carucci[a,1], A. Kurman[a,1], H. Karhu[b], K. Arve[a,1], K. Eränen[a,1], J. Wärnå[a,1], T. Salmi[a,1], D.Yu. Murzin[a,*]

[a] Laboratory of Industrial Chemistry and Reaction Engineering, Process Chemistry Centre, Åbo Akademi University, Biskopsgatan 8, FI-20500, Turku/Åbo, Finland
[b] Department of Physics and Astronomy, University of Turku, Vesilinnantie 5, FIN-20014, Turku, Finland

ARTICLE INFO

Article history:
Received 27 November 2008
Received in revised form 16 January 2009
Accepted 20 January 2009

Keywords:
HC-SCR
Microreactor
Biodiesel
Kinetic modelling

ABSTRACT

Catalytically active microchannels containing 1.5 wt.% Ag/alumina were used for studying the kinetics of the hydrocarbon-assisted selective catalytic reduction of NO_x. Hexadecane, a model component for second-generation biodiesels, was used as a reducing agent. Steady-state data from the microreactor was used to develop a detailed kinetic model. The kinetic parameters were estimated through numerical data fitting, with plug flow model for the microchannels. The model explained fairly well the experimental data.

1. Introduction

Microreactor technology has emerged as one of the most vigorous research areas during the past decade proven by the large amount of scientific publications in the field [1–5]. The benefits of these devices compared with conventional vessels are numerous: enormous improvements in energy efficiency allowing very high heat transfer rates; faster reactions, suppressing mass transfer limitations effects; improved yields due to the faster heat and mass transfer capabilities; intrinsic safety because of the small-channel dimensions, which gives reliability; and last but not least, a better process control is achieved [6–8]. These advantages make the microreactor an optimal set-up for obtaining fast and reliable kinetic data. Moreover, in previous studies, good agreements with results obtained in mini and microreactors under comparable conditions were obtained [9], making it possible to transfer results from mini to microreactors and vice versa.

Globally, there is a growing concern for the environment, and the strict legislations regarding emissions have led to an emerging research in the area of environmental catalysis. Nitrogen oxides are one of the most harmful compounds among these emissions, produced primarily from stationary (industry) and non-stationary (transport) sources during the combustion processes. Approximately 90% of the nitrogen oxides generated is in the form of nitric oxide (NO), which oxidizes rapidly to nitrogen dioxide (NO_2) in the presence of air. When these oxides react with water, nitric acid is formed which causes acidic rains.

For the case of diesel engines, which operate under a large excess of oxygen, the conventional three-way-catalyst approach cannot be employed and other techniques must be introduced. A SCR process for reducing NO_x using ammonia in stationary sources is well established. However, due to difficulties in storing and handling ammonia and its hazards for the potential user, it is not likely that this technology could be used in a passenger's vehicle. In principle, a safer component, i.e., urea could be used as a source of ammonia. In that case, the most promising catalyst has been found to be a vanadium-based one [10]. Even if the urea-SCR technology for NO_x removal employs urea instead of ammonia as a reductant, the process still produces NH_3 slip and problems with the infrastructure and distribution of the urea are a challenge to face [11]. A safer and more elegant approach to issue this problem is the hydrocarbon-assisted selective catalytic reduction (HC-SCR) of NO_x [12–18]. Since the pioneering work of Iwamoto et al. [12] and Held et al. [13], the exhaust treatment by HC-SCR of conventional fuels in diesel exhaust has been studied in detail in a large amount of industrial and academic publications. Iwamoto et al. [12] and Held et al. [13] investigated the activity of copper-exchanged zeolite ZSM-5 generating a great interest in the subject. However, the efforts put on Cu-ZSM-5 were limited due to the instability of this catalyst in the presence of water [14], making the following studies aimed towards non-zeolitic alternatives for the system. Noble metals supported on metal oxides have been tested obtaining promising results with short chain hydrocarbons, especially propene [14]. Pt was believed

* Corresponding author. Tel.: +358 22154431; fax: +358 22154479.
E-mail address: dmurzin@abo.fi (D.Yu. Murzin).
[1] Fax: +358 22154479.

1385-8947/$ – see front matter © 2009 Elsevier B.V. All rights reserved.
doi:10.1016/j.cej.2009.01.031

to be one of the best catalysts for the system as stated by Fritz and Pitchon in their review [18]. However, most of the recent development has been devoted to silver catalysts on alumina [19–26], since it has been found to be one of the most successful catalysts up to date [19]. The research has been focused on lower alkanes and alkenes as reductants, e.g., propene [14]. Still, there were some efforts on higher alkenes, i.e., octane [19] and even decane [20] and other more complex hydrocarbons [26]. Nevertheless, real on-board fuels, such as diesel, contain hundreds of compounds, usually higher alkanes than C_{10} [27].

On the other hand, biofuels are regarded as an alternative solution for reducing the oil dependence in the transport sector. According to the Directive 2003/30/EC of the European Parliament and of the Council, the European Union (EU) has set the use of biofuels to be of 5.75% of the total vehicle fuel consumption in the EU by 2010. In the case-scenario where biodiesel would substitute petrodiesel, the understanding of the NO_x reduction will be essential.

It has been previously proved that the HC-SCR NO_x reduction strongly depends on the nature of the hydrocarbon [28]. Although it is known that kinetics of a catalytic reaction can provide valuable information for catalytic converters design, and kinetic model for real exhaust treatment, there are surprisingly few papers in the literature describing kinetic studies for HC-SCR of NO_x with higher hydrocarbons (above C_{12}). The discussion has mainly been focused on lower hydrocarbons, e.g., propane [29], propene [30] and octane [31–33].

In this contribution, an attempt to close the gap is made: a systematic kinetic study for the selective catalytic reduction of NO_x with biodiesel is presented. It is based on the rigorous treatment of the chemical transformations occurring in selective catalytic reduction of NO_x in microchannels.

Neste oil has recently developed a process for the production of a biomass-derived diesel, called NExBTL, which consists mostly of C_{15}–C_{18} paraffins. Hexadecane, that can also be produced from renewable sources, i.e., vegetable oils by decarboxylation, and is regarded as a high-quality diesel [34,35], was selected as a model compound representing the second-generation biodiesels. Such green diesel is known for its renewability, biodegradability and fewer emissions (PM, SO_x, net CO_2, and VOC) in exhaust gases.

2. Experimental

2.1. Microreactor

The gas-phase microreactor set-up was constructed at Åbo Akademi and the parts were purchased from the Institut für Mikrotechnik Mainz GmbH (IMM). The device consists of a two-piece cubic chamber with two inlets and one outlet, each with a tube diameter of 710 μm. The lower part of the chamber has two recesses, each filled with a stack of 10 stainless steel (before the catalytic coating) micro-structured plates, which are connected by a diffusion tunnel, where the gases from the two reactor inlets mix before entering into the catalytic area. The first stack contains a total of 10 mixing plates with nine semicircular channels of different radii but with a common center. They are arranged in the stack in such a way that they meet the two inlets in alternation. The second stack consists of 10 rectangular plates with nine parallel shallow microchannels (Ø = 460 μm, length = 9.5 mm and depth = 75 μm) coated with an Ag/Al_2O_3 catalyst. Fig. 1 shows the microreactor chamber with the coated plates (left) as well as a scanning electron micrograph of the catalytically active channels (right).

2.2. Catalytic preparation and characterization

There is a need to introduce a catalytically active phase on the microchannels. The plates were previously coated with Al_2O_3 at IMM obtaining a mass of 0.7 mg per plate (7 mg total in the microchamber). The catalyst was further impregnated in our laboratory by washcoating with a 0.022 M aqueous silver nitrate solution of high purity (J.T. Baker). The impregnation time was 24 h and the stirring speed ca. 70 rpm. After impregnation, the platelets were dried at room temperature overnight and were further calcined in air for 3 h at 550 °C. More details of the procedure are described elsewhere [9]. The plates were further characterized by LA-ICP-MS [9] and X-ray photoelectron spectroscopy (XPS). A PerkinElmer 5400 ESCA spectrometer was used with monochromatized Al Kα radiation (photon energy 1486.6 eV) and a pass energy value of 35 eV. Samples were in contact with ambient air prior to analysis and the analysis was made from the surface of the microplate without any additional chemical or physical treatments. A low energy electron gun (flood gun) was used to stabilize the charging that arises from loss of photoelectrons during X-ray bombardment. To calibrate the binding energy axis accurately, carbon 1s line at 284.6 eV was used [36].

2.3. Kinetic experiments set-up

The kinetic experiments were carried out in the microreactor containing the previously coated plates. The microreactor chamber was connected to a temperature controller and thermocouples for monitoring the temperature in the catalytic area. The catalyst was pre-treated in a 6 vol.% O_2 flow in helium for 30 min. The experiments were carried out under atmospheric pressure and the temperature was varied from 150 to 550 °C (sampling every 50 °C). For each temperature, the concentrations of the reactants in the gas flow were varied as follows: (a) keeping the concentrations of hexadecane and oxygen at 187.5 and 60,000 ppm respectively, NO was

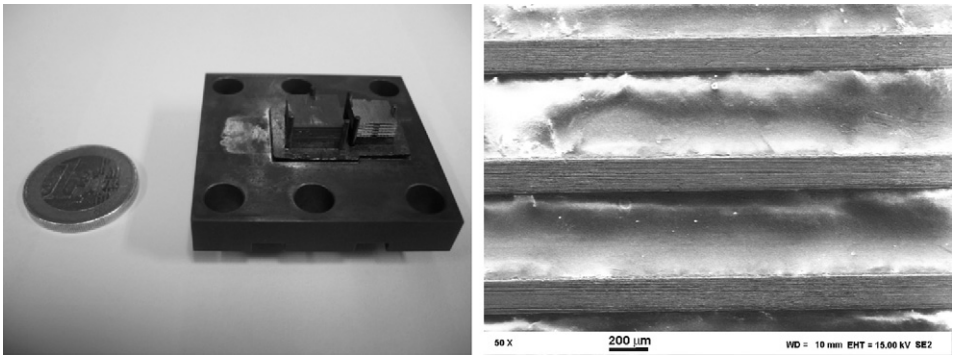

Fig. 1. Microreactor chamber with catalytic plates (left) and SEM picture of a coated microplate – 50× (right).

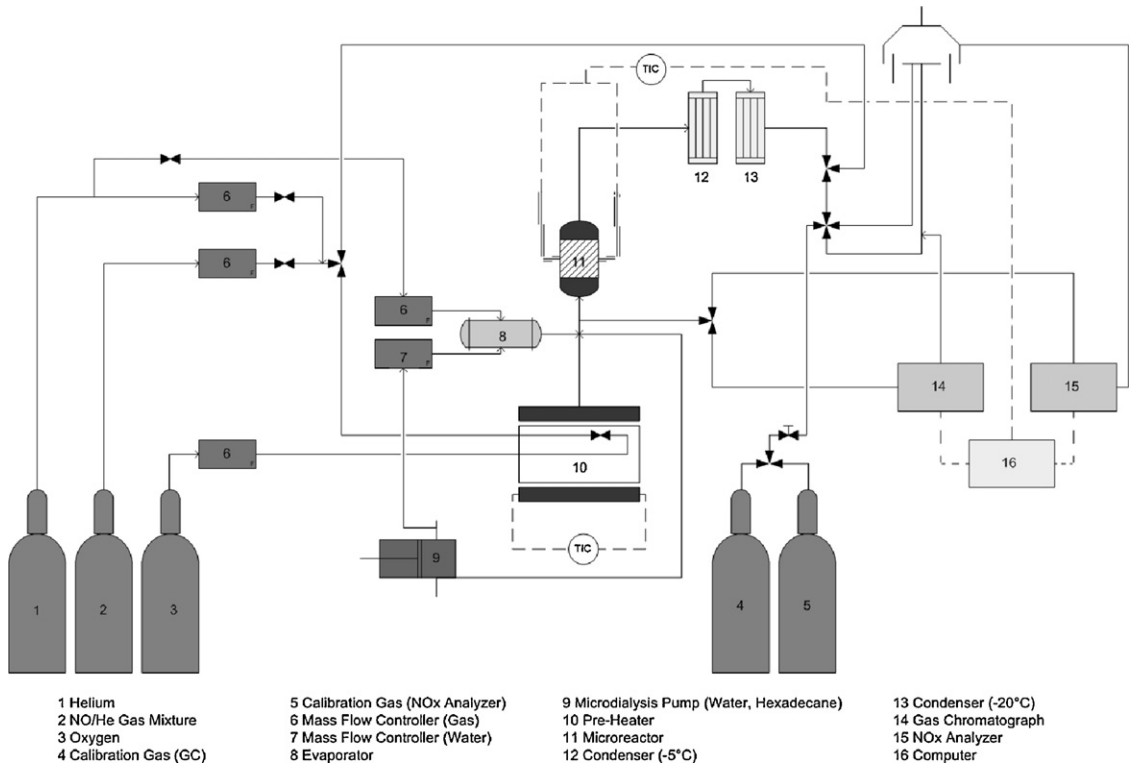

Fig. 2. Scheme of the experimental set-up.

varied (750, 1000, 1500, and 2000 ppm); (b) keeping the concentrations of NO and oxygen at 500 and 60,000 ppm, hexadecane was varied (187.5, 375, and 468.8 ppm); and (c) keeping the concentration of hexadecane and NO at 187.5 and 500 ppm, respectively, the oxygen variation was done (3, 4.5, 9, 12, and 15 vol.%). The concentration of water was kept constant at 12 vol.% in all the cases. It was used for balance. A total of 132 experiments were performed (12 different conditions at each temperature). The total gas-flow rate was always kept at 50 ml/min.

NO was fed from a mixture of 5.01 mol% NO in helium. All the gases were of high purity (AGA) and were pre-heated to 100 °C and introduced into the reactor by means of mass flow controllers (Brooks 5850).

The liquid flows, i.e., water and hexadecane, were pumped via a syringe pump (CMA/102 Microdialysis). Due to the small amounts of hexadecane present during the experiments (187.5–468.8 ppm), it was assumed that it was vaporised on the gas stream even at temperatures lower than its boiling point (287 °C). The liquids were condensed after the reactor, before gases were introduced to the gas chromatograph.

The concentrations of the resulting species were determined by a Hewlett-Packard Gas Cromatograph (GC) System 6890 series with TC an FI detectors, and the NO_x, NO and NO_2 concentrations were measured by a PPM Systems Chemiluminescent NO_x Analyzer model 200AH. High-purity calibration gases (AGA) were used for calibration of the NO_x analyzer and the GC. A scheme of the experimental set-up is presented in Fig. 2.

3. Results and discussion

3.1. Catalysts characterization

The metal uptake was measured by both LA-ICP-MS and XPS. The results of the latter are presented here. Fig. 3 shows the silver 3d line for one of the fresh-coated microplates. In most metals electron donation from metal to ligand is observed as increased binding energy. Silver does not follow this trend; binding energies of 368.3, 367.5 and 367.3 eV are found in metallic silver, AgO_2 and AgO respectively [36]. Silver nanoparticles dispersed over alumina also have a tendency towards electric charging during the analysis, which leads into calibration issues [37]. Despite the anomalous core-level chemical shifts in silver, binding energies of silver atom nanoclusters dispersed over alumina behave as platinum clusters;

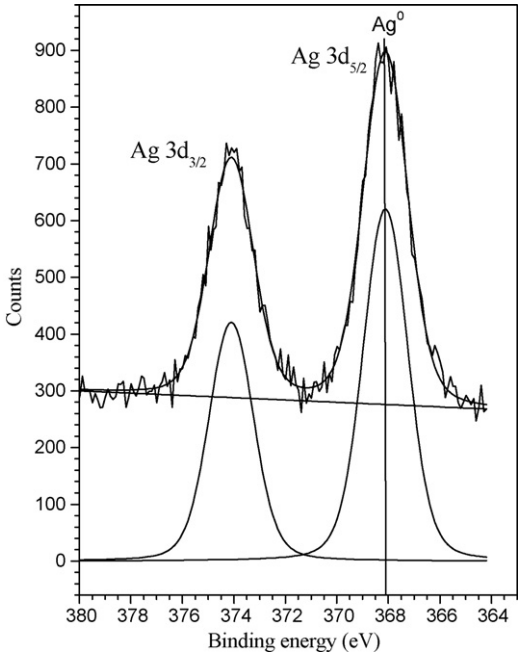

Fig. 3. Ag 3d line from the catalytically active microplate.

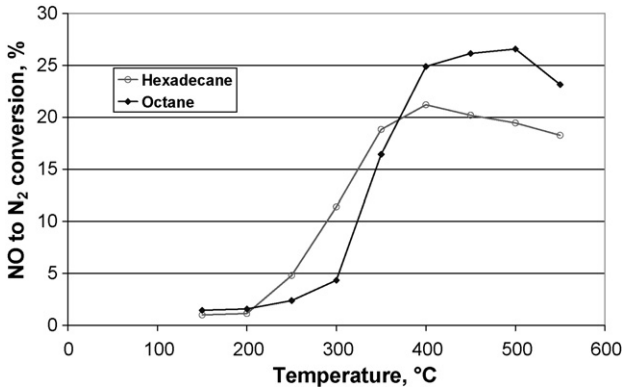

Fig. 4. NO to N_2 conversion on the HC-SCR over a 1.5 wt.% Ag/alumina microchannel with hexadecane (-◯-) and octane (-♦-). 500 ppm NO, C1/NO = 6, 6 vol.% O_2, 12 vol.% H_2O and He balance. Total flow 50 ml/min.

very small Ag particles have a binding energy that is ca. 0.9 eV higher than bulk Ag 3d5/2 [38]. Although it is not easy to determine the oxidation state of the silver over the alumina support, the XPS binding energy (368.1 eV, with C 1s at 284.6 eV) suggests that silver was in the Ag^0 form and the average particle diameter is at least a few nanometers. The silver loading was found to be 1.5 wt.% with respect to the alumina and the B.E.T. specific surface area, according to the manufacturer was found to be 70 m^2/g before the metal impregnation [39].

3.2. Activity tests

The NO to N_2 conversion of the hexadecane-assisted SCR over a 1.5 wt.% Ag/alumina-coated microchannels is shown in Fig. 4. The reduction conversion with octane is used for comparison purposes, as a representative component for fossil fuels, on the same microreactor. Even though the utilization of octane results in the highest NO-to-N_2 conversion, the low-temperature activity improvement of hexadecane (<350 °C) is significant. At 350 °C, the NO reduction with $C_{16}H_{34}$ is four times higher than in the case of C_8H_{18}. Theoretical studies of n-alkanes on metal surfaces suggest that the adsorption energies increase linearly with the chain length [40,41]. The greater enthalpy of adsorption of the longer alkane chains and the weaker C–H bond strength of their methylene groups could at least partially explain their greater ability to react at lower temperatures. On the other hand, the geometry of the molecule could have an effect on its reactivity. Hexadecane, with its larger size compared to octane, would occupy more space when adsorbed on a metal cluster. Thus, due to steric hindrance, less available space would be available for other molecules to adsorb, e.g., NO. In any case, the reduction behaviour and reaction mechanism is expected to be similar for both cases.

The two main reactions in the hydrocarbon assisted-SCR are the NO reduction and the hydrocarbon oxidation. In the present case they are represented by Eqs. (1) and (2)

$$2NO + C_{16}H_{34} + 23.5O_2 \rightarrow N_2 + 16CO_2 + 17H_2O \quad (1)$$

$$C_{16}H_{34} + 24.5O_2 \rightarrow 16CO_2 + 17H_2O \quad (2)$$

It is generally assumed that reactions (1) and (2) are connected, and that Eq. (1) cannot occur if the hydrocarbon is not partially oxidized.

3.3. NO effect

The effect of NO initial concentration 500–2000 ppm on the NO to N_2 reduction and the $C_{16}H_{34}$ to CO_2 + CO oxidation, over Ag/Al_2O_3 at different temperatures (150–550 °C) is shown in Fig. 5. A clear tendency of decreasing the reduction activity (Fig. 5a), as well as the oxidation one (Fig. 5b) was observed. Regarding the reduction activity (Fig. 5a), at lower temperatures (<250 °C), despite a slight decrease on the conversion when higher NO concentrations are injected, the negative slope is not very pronounced. It is clear that the activation of the hydrocarbon does not occur at these temperatures, which also impedes the reduction activity. At temperatures above 300 °C, the inhibiting effect of NO started to appear. A possible explanation would be that at very high concentrations of NO, the active silver sites are blocked by the adsorption of these species, not letting the hydrocarbon to adsorb. As it is conventionally assumed, the adsorption of the hydrocarbon is a necessary step for the reduction to occur. More details can be found below when the reaction mechanism is discussed. A similar tendency has been previously reported by Shimizu et al. for SCR of NO_x with propane in minireactors [42].

The addition of even more NO at the inlet ([NO] > 1400 ppm) does not affect strongly the conversion. It seems that as more NO is introduced into the system, it would only contribute to the bulk concentration, without affecting the catalytic activity of the already filled active sites; hence, not changing the NO to N_2 activity in great extent.

It is not surprising that the behaviour of the oxidation of the hydrocarbon follows the same trend (Fig. 5b). In this case, even at temperatures below 250 °C, the inhibiting effect of the NO concentration is depicted. However, the negative effect, for the oxidation of hexadecane, tends to increase with the augment of temperature. In a parallel study of the hexadecane-SCR of NO_x in minireactors (diameter 10 mm), a similar behaviour was found, even at smaller NO concentrations (up to 100 ppm). In this study, a maximum of NO to N_2 conversion was observed with a NO initial concentration of 250 ppm [43]. Studies with other hydrocarbons, e.g., propane, have shown the same pattern [42].

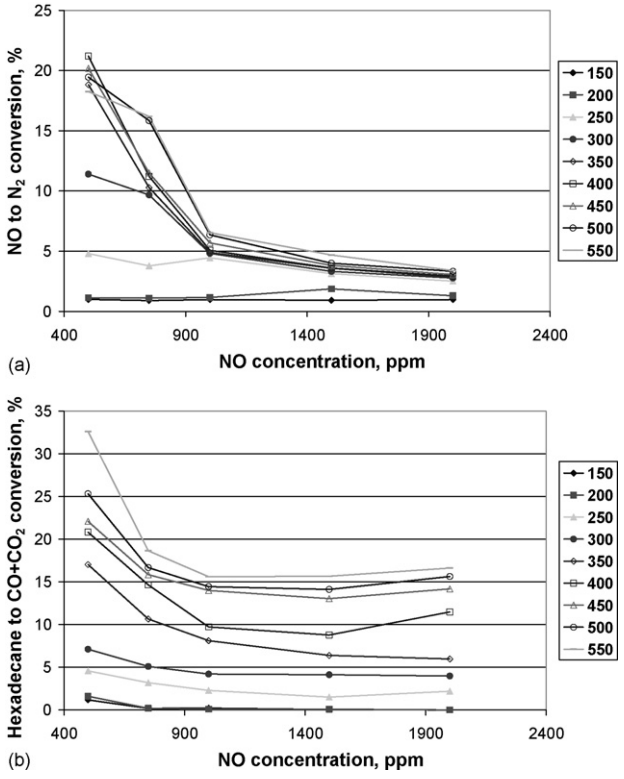

Fig. 5. (a) NO reduction and (b) hexadecane oxidation over a 1.5 wt.% Ag/alumina microchannel varying NO partial pressure. 150 °C (-♦-); 200 °C (-■-); 250 °C (-▲-); 300 °C (-●-); 350 °C (-◇-); 400 °C (-□); 450 °C (-△-); 500 °C (-◯-); 550 °C (---). 187.5 ppm $C_{16}H_{34}$, 6 vol.% O_2, 12 vol.% H_2O and He balance. Total flow 50 ml/min.

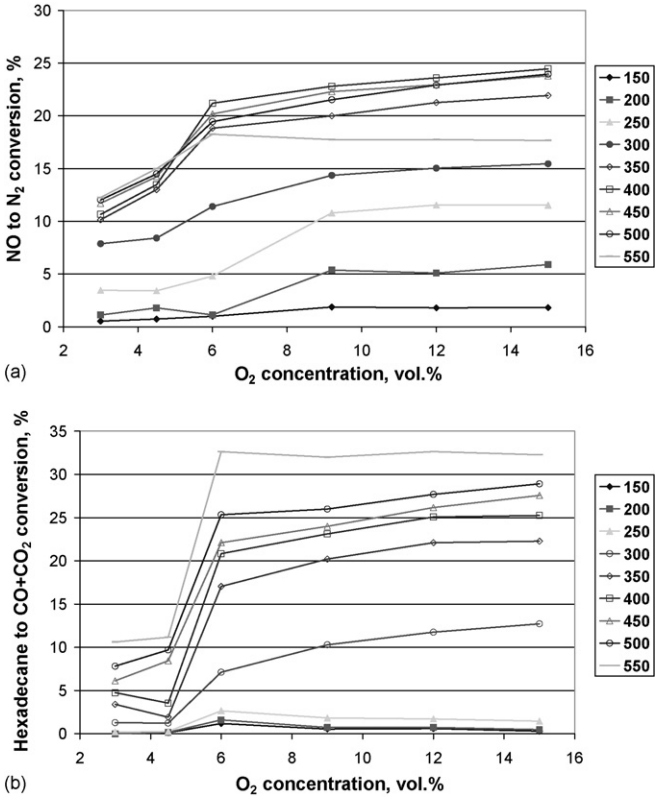

Fig. 6. (a) NO reduction and (b) hexadecane oxidation over a 1.5 wt.% Ag/alumina microchannel varying O_2 partial pressure. 150 °C (-♦-); 200 °C (-■-); 250 °C (-▲-); 300 °C (-●-); 350 °C (-◊-); 400 °C (-□); 450 °C (-△-); 500 °C (-○-); 550 °C (---). 500 ppm NO, 187.5 ppm $C_{16}H_{34}$, 12 vol.% H_2O and He balance. Total flow 50 ml/min.

3.4. O_2 effect

Fig. 6 presents the effect of oxygen initial concentration on the NO to N_2 reduction and the $C_{16}H_{34}$ to CO_2 + CO oxidation. An increase in reduction activity (Fig. 6a) is observed when higher concentrations of oxygen were fed into the system. Previous studies have found Ag/alumina catalyst to be active in excess of oxygen [15]. For lower temperatures (below 300 °C), the NO reduction reached an inflexion point around 9 vol.% of O_2 initial concentration. A further increase in the oxygen concentration resulted in the same reduction activity. For the case of higher temperatures (above 300 °C), the inflexion point was found to be around 6 vol.% of initial concentration of oxygen, at higher concentrations, the NO to N_2 conversion did not increase very sharply. The curves followed an S-shape behaviour found previously by other authors, with other hydrocarbons, i.e., propane [42], propene [44] and decane [45].

For the oxidation of the hydrocarbon case (Fig. 6b), the inflexion point is more pronounced. However, both the oxidation and the reduction trends seem to be the same, which suggests that the activation of the hydrocarbon plays an important role in the mechanism for the hexadecane-SCR over Ag/alumina. An assumption that the adsorption of the hydrocarbon and its partial oxidation is an essential step in the conversion of NO to N_2, is in line with these results.

Again, at oxygen concentrations close to 15 vol.%, the increase of oxygen in the feed stream becomes unimportant and the reduction and oxidation cease to increase.

3.5. $C_{16}H_{34}$ effect

The dependence of the reduction activity and oxidation on the concentration of the reducing agent, hexadecane, is depicted in Fig. 7.

For the case of NO reduction (Fig. 7a), an interesting behaviour was observed. At lower temperatures, a lower C1 to NO ratio seems to enhance the reduction of NO. Nevertheless, at higher temperatures, the effect is the opposite, i.e., higher concentrations of hexadecane result in the augment of the catalytic activity.

This interesting behaviour has not been reported for either short or long-chained paraffins. Previous studies with octane suggested that the hydrocarbon had only a positive effect on the NO to N_2 reduction [46]. When increasing the concentration of hexadecane, hence, its coverage raises, it could be that the molecule would impede the adsorption of the nitrogen oxide on the catalyst, inhibiting the NO reduction reaction (Fig. 7a). On the other hand, the oxidation conversions follow the same pattern: there is a detrimental effect when adding more hexadecane in the feed at lower temperatures (below 350 °C), while the behaviour was reversed at temperatures above 350 °C (Fig. 7b). The measured data on the minireactor and further rate calculations based on it [46] suggested that hexadecane did not limit the oxygen coverage on the surface, since the oxidation rates were promoted by higher concentrations of the hydrocarbon, even for the cases when the NO to N_2 reduction rates were inhibited [46]. At temperatures above 350 °C, the hexadecane was not inhibiting anymore the SCR since the oxidation rate was very high, indicating lower hexadecane coverage in the high temperature range, helping to promote the NO to N_2 reduction. Although the conversion values were not identical for the micro and minireactor systems, the trends were found to agree.

In brief, the inhibition of the nitrogen oxides adsorption on the surface as previously mentioned could be the explanation for the reduction of the NO to N_2 conversion with high hexadecane concentrations. Moreover, the larger size of the hexadecane molecule compared with previously studied molecules, i.e., octane, could

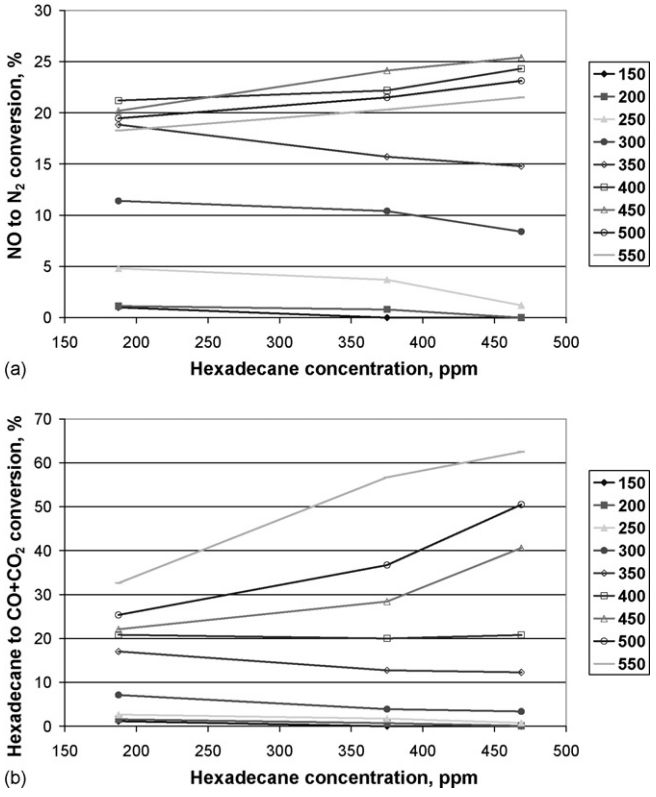

Fig. 7. (a) NO reduction and (b) hexadecane oxidation over a 1.5 wt.% Ag/alumina microchannel varying $C_{16}H_{34}$ partial pressure. 150 °C (-♦-); 200 °C (-■-); 250 °C (-▲-); 300 °C (-●-); 350 °C (-◊-); 400 °C (-□); 450 °C (-△-); 500 °C (-○-); 550 °C (---). 500 ppm NO, 6 vol.% O_2, 12 vol.% H_2O and He balance. Total flow 50 ml/min.

influence its adsorption mode. It would take more space on the active sites than smaller molecules.

This effect could presumably be explained by the coverage of the active sites on the catalyst. When increasing the amount of the hydrocarbon, it would saturate the catalytic surface, impeding other molecules to adsorb and resulting on a decrease of the reduction activity as it was experimentally observed.

Then, since the boiling point of hexadecane is quite high (287 °C) even with very small amounts of this compound in the gas mixture (187.5–468.8 ppm), some condensation of the component on the surface might occur, ceasing the oxidation of the hydrocarbon, a key step on the SCR. The condensation of the hydrocarbon would imply the diffusion of the reactants through the liquid film (slower than the diffusion through the gas phase) and limiting the adsorption of the species present in the reaction. This phenomenon could also affect the way the different species are adsorbed on the surface.

This explanation, although feasible, would not be sufficient to explain the reduction of NO to N_2 activity, since a similar effect was demonstrated with other components with lower boiling points, i.e., aromatics in [47]. A more plausible explanation would be the inhibition of the NO adsorption due to hexadecane molecule size, as was also found in a similar system in minireactors [46].

As mentioned before, the effect of hexadecane at temperatures above 350 °C was the opposite, i.e., higher concentrations of the paraffin resulted in NO-to-N_2 activity improvements. At sufficiently high temperatures, no hexadecane liquid film is present on the surface, giving other molecules the possibility to adsorb on the catalytic layer.

In general, due to the relatively small amount of available active sites in the microchannels, when the reactants concentrations in the feed stream tend to increase, it is presumed that the reactive species: oxygen, NO and hexadecane compete for adsorbed sites and to react further to intermediates, which will eventually react among them to produce molecular nitrogen.

Although Houel et al. [48] proposed coking on Ag/alumina catalyst as the underlying cause for the decrease of the reduction activity at low temperatures when using dodecane as reducing agent, no evidences of deactivation could be found in the present study.

4. Reaction mechanism

Based on the kinetic data from the performed experiments and with previously published mechanism of the SCR for different hydrocarbons, a reaction mechanism for $C_{16}H_{34}$-SCR of NO_x over Ag/alumina microchannels was proposed. Principally, it follows the mechanism published by our group [32] and considerations presented in [49]. The reaction mechanism is given in Table 1, with 21 reaction steps and 9 reaction routes. The stoichiometric numbers are presented as well, and they were chosen in a way that no intermediates would appear in the overall equations for each route.

Molecular adsorption of NO and CO are assumed, as well as dissociative adsorption of O_2 [32]. While Backman et al. [32] proposed a mechanism for H_2-assisted HC-SCR of NO_x, it was also stated that the mechanism was similar as in the absence of hydrogen. It is assumed here that the behaviour of a higher hydrocarbon, i.e., hexadecane, will be analogous as the one obtained with octane as a reducing agent, with some differences based on our kinetic observations that will be explained below.

It is generally agreed that over Ag/alumina catalysts, the reduction of NO proceeds through a complex reaction network. It is suggested that the role of the catalyst in this case is to oxidize the hydrocarbon to O- and N-containing intermediate compounds, which will further react with NO to produce molecular nitrogen [23].

According to the experimental data (see Section 3 above) conversions in the $C_{16}H_{34}$ oxidation were higher than the NO to N_2 reduction (Figs. 5–7).

It was then suggested that oxidation of the hydrocarbon is a first step leading to strongly bound intermediates that react with pre-adsorbed nitrite or nitrate moieties: chemisorption of the hydrocarbon via pre-adsorbed oxygen is proposed, which further splits the C–H bond, resulting in adsorbed hydrocarbon specie and a hydroxyl group (step 8). The adsorbed hydrocarbon will then react either with a previously adsorbed NO to produce a N-functionalized hydrocarbon intermediate (HC–NO), as suggested previously in the literature (step 9) [23], or with another adsorbed oxygen to produce oxygenated hydrocarbons (step 12). Molecular nitrogen is suggested to be formed either by the combination of two of the

Table 1
Proposed mechanism and routes, of the $C_{16}H_{34}$-SCR of NO over Ag/Al_2O_3-coated microchannels.

Step	Reaction	$N^{(1)}$	$N^{(2)}$	$N^{(3)}$	$N^{(4)}$	$N^{(5)}$	$N^{(6)}$	$N^{(7)}$	$N^{(8)}$	$N^{(9)}$
1	$NO+^* \Leftrightarrow NO^*$	0	0	1	1	1	1	0	1	1
2	$NO^* + ^* \rightarrow N^* + O^*$	0	0	0	0	0	0	0	−1	0.5
3	$O_2 + 2^* \Leftrightarrow 2O^*$	49	33	24	16	23	15	0.5	0.5	0
4	$2N^* \rightarrow N_2 + 2^*$	0	0	0	0	0	0	0	−1	0
5	$NO^* + O^* \rightarrow NO_2 + 2^*$	0	0	0	0	0	0	0	1	0
6	$CO + ^* \Leftrightarrow CO^*$	0	−32	0	−16	0	−16	1	0	1
7	$CO^* + O^* \rightarrow CO_2 + 2^*$	32	0	16	0	16	0	1	0	0.5
8	$C_{16}H_{34} + O^*+^* \rightarrow C_{16}H_{33}{}^* + OH^*$	2	2	1	1	1	1	0	0	0
9	$C_{16}H_{33} + NO^* \rightarrow C_{16}H_{33}NO^* + ^*$	0	0	1	1	0	0	0	0	0
10	$2C_{16}H_{33}NO^* \rightarrow N_2 + 2C_{16}H_{33}O^*$	0	0	0.5	0.5	0	0	0	0	0
11	$C_{16}H_{33}O* + 48O* \xrightarrow{fast} 16CO* + 33OH*$	2	2	1	1	1	1	0	0	0
12	$C_{16}H_{34}{}^* + O^* \rightarrow C_{16}H_{33}O^* + ^*$	2	2	0	0	0	0	0	0	0
13	$2OH^* \rightarrow H_2O + O^*$	34	34	17	17	17	17	0	0	0
14	$C_{16}H_{33}NO^* + NO^* \rightarrow N_2 + C_{16}H_{33}O^* + O^*$	0	0	0	0	1	1	0	0	0
15	$NO_2 + ^* \Leftrightarrow NO_2{}^*$	0	0	0	0	1	1	0	0	0
16	$C_{16}H_{33}{}^* + NO_2{}^* \rightarrow C_{16}H_{33}NO^* + O^*$	0	0	0	0	1	1	0	0	0
17	$N^* + CO^* \rightarrow NCO^*$	0	0	0	0	0	0	0	0	0.5
18	$NCO* + H_2O \xrightarrow{fast} NH_2* + CO_2$	0	0	0	0	0	0	0	0	0.5
19	$NH_2{}^* + NO^* \rightarrow H_2O$	0	0	0	0	0	0	0	0	0.5
20	$N^* + NO^* \rightarrow N_2O^* + ^*$	0	0	0	0	0	0	0	1	0
21	$N_2O* \xrightarrow{fast} N_2 + O*$	0	0	0	0	0	0	0	1	0

$N^{(1)}$: $2C_{16}H_{34} + 49O_2 \rightarrow 32CO_2 + 34H_2O$; $N^{(2)}$: $2C_{16}H_{34} + 33O_2 \rightarrow 32CO_2 + 34H_2O$; $N^{(3)}$: $C_{16}H_{34} + NO + 24O_2 \rightarrow 16CO_2 + 17H_2O + 0.5N_2$; $N^{(4)}$: $C_{16}H_{34} + NO + 16O_2 \rightarrow 16CO + 17H_2O + 0.5N_2$; $N^{(5)}$: $C_{16}H_{34} + NO + NO_2 + 23CO_2 \rightarrow 16CO_2 + 17H_2O + N_2$; $N^{(6)}$: $C_{16}H_{34} + NO + NO_2 + 15O_2 \rightarrow 16CO + 17H_2O + N_2$; $N^{(7)}$: $CO + 0.5O_2 \rightarrow CO_2$; $N^{(8)}$: $NO + 0.5O_2 \rightarrow NO_2$; $N^{(9)}$: $NO + CO \rightarrow 0.5N_2 + CO_2$.

HC–NO species (step 10) or by the reaction between a HC–NO intermediate and a pre-adsorbed NO (step 14). Both steps would also form oxygenated hydrocarbons, which are considered to rapidly react with adsorbed oxygen to produce adsorbed CO and OH (step 11).

It has been suggested that CO_2 is formed through CO [31]. According to Klingstedt et al. [25] a drawback of the Ag/alumina catalyst is its poor catalytic activity at low temperatures (below 300 °C) and the strong CO formation for the octane-SCR. They also attributed the formation of CO_2 to the further oxidation of the adsorbed CO, likely to be enhanced at high temperatures as it was experimentally proved. CO is suggested to be formed when oxygenate species rapidly react with adsorbed oxygen to form surface CO and hydroxyl (step 11). Surface CO can be further oxidized to CO_2 reacting with adsorbed oxygen (step 7), or it could also react with adsorbed nitrogen to produce adsorbed isocyanate (step 17).

Isocyanates are likely to be formed in the lower temperature range. When using octane the low temperature SCR of NO_x (<350 °C) is not very effective [50], hence its elementary steps were discarded [32]. However, when hexadecane is used as a reducing agent, low temperature activity tends to increase (see Fig. 4) and isocyanate species are likely to appear. Burch [49] indicated that –NCO species were remarkably stable except when a very high concentration of NO was introduced. On the other hand, he also stated that the rate of reaction of the –NCO species with NO under more typical HC-SCR conditions, e.g., the ones used in this work, might be too slow to contribute significantly to the formation of N_2. Nevertheless, we have included these steps in our model, again, for a generalization of the system.

Steps 11, 18 and 21 are considered fast. These three reactions are obviously not elementary surface reactions [51]. They involve two or more elementary steps, thus the surface coverage of $C_{16}H_{33}O^*$, NCO* and N_2O^* was considered negligible.

Under lean conditions, the selectivity in the reduction of NO to either N_2 or N_2O has been found to be favoured towards the latter at low temperatures [49]. Moreover, Denton et al. [52] concluded that N_2O was in fact, an intermediate in the reduction of NO to N_2 at temperatures higher than 230 °C [52].

Additionally, relatively high yields of NO_2 can be obtained by the oxidation of organo-nitrito compounds, and hence, formation of NO_2 was also taken into account (step 5). Nevertheless, NO_2 is more reactive than NO and as a result it may adsorb in order to form ad-NO_x species. The experiments evidenced the production NO_2 in all the temperature range opposite to what was found for the case of octane [31].

With these considerations, the proposed reaction mechanism is presented in the already mentioned in Table 1.

Regarding the 9 reaction routes, $N^{(1)}$ and $N^{(2)}$ are the complete and partial oxidation of the hexadecane, while $N^{(3)}$ and $N^{(4)}$ correspond to the reduction of NO. Routes $N^{(5)}$ and $N^{(6)}$ describe the complete and partial HC-SCR with the presence of reacting NO_2. Routes $N^{(7)}$ and $N^{(8)}$ account for the basic mechanism for the formation of CO_2 and NO_2 and route $N^{(9)}$ deals with the isocyanate pathway.

Only reactions occurring on the catalytic surface were considered. Mass transfer restrictions were supposed to be negligible. Due to the dimensions of the microchannels (230 μm of radius on its larger part), the mass transfer between the gaseous species and the catalytic layer is sufficiently high.

5. Rate equations

In order to properly analyze the complex reaction system elementary reactions were proposed. A linear combination of elementary steps, multiplied by the corresponding stoichiometric number were grouped into reaction routes. The total number of reaction routes was determined by the expression proposed by Horiuti and further developed by Temkin [53]. The concentrations of the adsorbed intermediates were expressed as surface coverages (θ_i), according to the ideal case of chemisorption on surface reactions developed by Langmuir [51]. The quasi-equilibrium approximation was assumed for the adsorption of the reactants, Eqs. (3)–(6):

$$\theta_{NO} = K_1 c_{NO} \theta_v \tag{3}$$

$$\theta_{O} = \sqrt{K_3 c_{O_2}}\,\theta_v \tag{4}$$

$$\theta_{CO} = K_6 c_{CO} \theta_v \tag{5}$$

$$\theta_{NO_2} = K_{15} c_{NO_2} \theta_v \tag{6}$$

where K_i represents the equilibrium constant, accounting for the adsorption strength of each species. The formation of NO_2 was observed when hexadecane was applied as a reducing agent, contrary to the case when octane is used [31], hence, it was included on the mechanism. When deriving the equations, the concentrations of surface intermediates were assumed to be at steady-state, meaning that the sum of the rates of formation of surface intermediates in elementary reactions is equal to the sum of the rates of its consumption in other elementary steps.

For instance, for $C_{16}H_{33}{}^*$ it follows that:

$$r_8 = r_9 + r_{12} + r_{16} \tag{7}$$

Substituting each corresponding rate expressions in Eq. (7):

$$k_8 c_{hex} \theta_O = k_9 \theta_{hex} \theta_{NO} + k_{12} \theta_{hex} \theta_O + k_{16} \theta_{hex} \theta_{NO_2} \tag{8}$$

Solving for c_{hex}, and introducing Eqs. (3), (4) and (6); an expression for the hexadecane coverage ($C_{16}H_{33}{}^*$) is obtained:

$$\theta_{hex} = \frac{k_8 c_{hex} \sqrt{K_3 c_{O_2}}}{k_9 K_1 c_{NO} + k_{12} \sqrt{K_3 c_{O_2}} + k_{16} K_{15} c_{NO_2}} \times \theta_v \tag{9}$$

With the same procedure, coverages for other species could be obtained. In the cases where more than one solution was possible (quadratic expressions), the only solution with physical meaning was considered ($0 < \theta_i < 1$).

For hexadecane-NO ($C_{16}H_{33}NO^*$) it follows that:

$$r_9 = 2r_{10} + r_{14} - r_{16} \tag{10}$$

which is then:

$$k_9 \theta_{hex} \theta_{NO} = 2k_{10} \theta_{hex\text{-}NO}^2 + k_{14} \theta_{hex\text{-}NO} \theta_{NO} - k_{16} \theta_{hex} \theta_{NO_2} \tag{11}$$

resulting in an expression for the coverage of the specie $C_{16}H_{33}NO^*$:

$$\theta_{hex\text{-}NO} = \left(\frac{-k_{14} K_1 c_{NO} + \sqrt{k_{14}^2 K_1^2 c_{NO}^2 + 8 k_{10} k_8 c_{hex} \sqrt{K_3 c_{O_2}} \left(k_9 K_1 c_{NO} + k_{16} K_{15} c_{NO_2} / k_9 K_1 c_{NO} + k_{12} \sqrt{K_3 c_{O_2}} + k_{16} K_{15} c_{NO_2} \right)}}{4 k_{10}} \right) \theta_v \tag{12}$$

Analogously, using the steady state approximation for the intermediate hydroxyl (OH*):

$$r_8 = 2r_{13} \tag{13}$$

which leads to:

$$\theta_{OH} = \left(\sqrt{\frac{k_8 c_{hex} \sqrt{K_3 c_{O_2}}}{2 k_{13}}} \right) \theta_v \tag{14}$$

and nitrogen (N*):

$$r_2 = 2r_4 + r_{17} - r_{20} \quad (15)$$

yielding an expression for the coverage of this species:

$$\theta_N = \left(\frac{-k_{17}K_6c_{CO} - k_{20}K_1c_{NO} + \sqrt{(k_{17}K_6c_{CO} + k_{20}K_1c_{NO})^2 + 8k_4k_2K_1c_{NO}}}{4k_4} \right) \theta_v \quad (16)$$

Since the number of sites is assumed to be equal to unity, the following balance equation is proposed (Eq. (17)), from which the surface coverage of vacant sites can be calculated

$$\theta_v + \theta_{NO} + \theta_O + \theta_{CO} + \theta_{NO_2} + \theta_{hex} + \theta_{hex\text{-}NO} + \theta_{OH} + \theta_N = 1 \quad (17)$$

It is important to notice that, as deduced from Eq. (17), only one type of metal site on the catalytic surface was considered. In principle, it is possible that different oxidation states of silver (Ag^0, Ag^+, etc.) could be present in the system. In situ spectroscopy studies would be needed in order to validate and determine the oxidation states of the metal before, during and after the reaction.

Each route of the reaction could be expressed as a linear combination of runs along the basic routes [54]. Under this premise, the rates of production or consumption for different species are presented in Eqs. (18)–(21).

Hexadecane is consumed along the routes $N^{(1)}$, $N^{(2)}$, $N^{(3)}$, $N^{(4)}$, $N^{(5)}$, and $N^{(6)}$, giving its rate of consumption as follows:

$$-r_{hex} = \frac{r_{12}}{2} + \frac{r_{12}}{2} + \frac{r_{10}}{0.5 \times 2} + \frac{r_{10}}{0.5 \times 2} + r_{14} + r_{14} = r_{12} + 2r_{10} + 2r_{14} \quad (18)$$

Analogously the rates of consumption of nitric oxide, consumed along routes $N^{(3)}$, $N^{(4)}$, $N^{(5)}$, $N^{(6)}$, $N^{(8)}$, and $N^{(9)}$ is given by:

$$-r_{NO} = \frac{r_{10}}{0.5 \times 2} + \frac{r_{10}}{0.5 \times 2} + \frac{r_{14}}{2} + \frac{r_{14}}{2} + r_5 + \frac{r_{19}}{0.5} = 2r_{10} + r_{14} + r_5 + 2r'_{19} \quad (19)$$

Since adsorbed NH_2 is generally assumed to be very reactive specie in the SCR of NO_x [27], its coverage was considered negligible and Eq. (19) could be further simplified ($r_{19} \approx 0$) into Eq. (20)

$$-r_{NO} = 2r_{10} + r_{14} + r_5 \quad (20)$$

Analogously the rates of production of molecular nitrogen could also be obtained. The expression becomes:

$$r_{N_2} = 4r_{10} + 2r_{14} \quad (21)$$

6. Parameter estimation

In order to understand the catalytic behaviour and the mechanisms involved in complex chemical systems, e.g., HC-SCR of NO_x, kinetic studies, as well as reactor models, should be developed. The kinetic modelling and parameter estimation performed in this work are based on the experimental data obtained in the activity experiments (Section 3). Isothermal plug flow model was used for each studied temperature. The kinetic data was simultaneously fitted by non-linear regression to the rate equations as a function of the independent variables: concentrations of $C_{16}H_{34}$, NO, NO_2, CO, CO_2, H_2O and O_2 that were measured at the inlet and outlet of the microreactor. The model predictions and kinetic parameters were obtained by using the parameter estimation software ModEst 6.0 [55]. A stiff ODE-solver (Odessa) with the Simplex-Levenberg–Marquardt algorithm implemented in the software was used to solve the system. The sum of residual squares was minimized using the following objective function (Eq. (22)):

$$Q = \left\| c_{exp} - c_{est} \right\|^2 = \sum_t \sum_i (c_{exp,it} - c_{est,it})^2 \quad (22)$$

The degree of explanation that represented the accuracy of the fit was given by Eq. (23):

$$R^2 = 100 \times \left(1 - \frac{\left\| c_{exp} - c_{est} \right\|^2}{\left\| c_{exp} - \bar{c}_{exp} \right\|^2} \right) \quad (23)$$

where $\bar{c}_{exp}$ represents the mean value of all the data points. In the model, the temperature dependences of the rate constants were expressed as in Eq. (24):

$$k_i = A_{i,ave} \times \exp\left(\frac{-Ea_i}{R} \left(\frac{1}{T_{Rx}} - \frac{1}{T_{ave}} \right) \right), \quad \text{with}$$

$$A_{i,ave} = A \times \exp\left(\frac{-Ea}{R \times T_{ave}} \right) \quad (24)$$

The estimated parameters are presented in Table 2.

Due to the numerical stiffness of the problem, good initial estimates are crucial for convergence. Previously found values in minireactors for octane-SCR from different publications [31] have been employed as initial estimates in the present work.

In this first stage of parameter estimation no simplifications for the model were made following the ambitious aim of creating a kinetic model that fully describes the hexadecane-SCR of NO_x over Ag/alumina, even if the system is very complex and the standard errors would be significant in this first attempt.

Despite of the large number of parameters, the model was successfully fitted to the experimental data with a high degree of explanation (≈95%, Eq. (23)). The comparison between experimental data and calculated values is given in Fig. 8. Even if there are values that differ, the proposed model was fitting the data with a good degree of accuracy.

However, in these types of systems, problems of overparametrization could occur. In order to discard this possibility, sensitivity analysis was applied. Sensitivity plots of two of the parameters A_2 (Fig. 9a) and A_{12} (Fig. 9b) are presented in Fig. 9. The behaviour of most of the estimated parameters was similar, obtaining a minimum of the objective function close to the estimated value. A simplified model with less parameter could be proposed for future contributions in order to diminish the standard errors and the overall explanation factor.

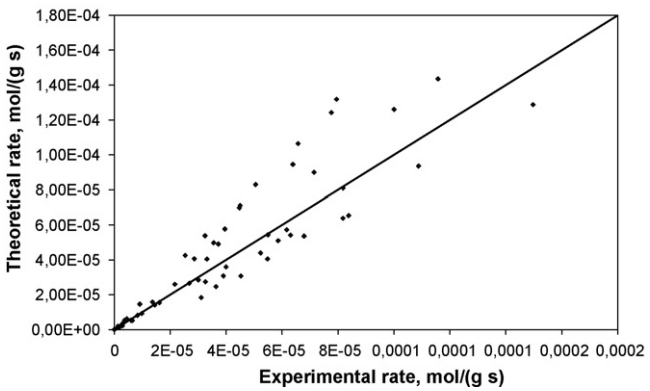

Fig. 8. Comparison between experimental and predicted reaction rate.

Table 2
Parameters from the fitting of the experimental data using non-linear regression.

Pre-exponential factor	Estimated values ($ppm^{-1}\ s^{-1}$)	Activation energy	Estimated values (kJ/mol)
A_2	$(8.97 \pm 1.08) \times 10^9$	Ea_2	112.1 ± 5.2
A_4	$(8.12 \pm 3.04) \times 10^4$	Ea_4	78.5 ± 49.3
A_5	$(2.73 \pm 1.31) \times 10^0$	Ea_5	37.9 ± 12.9
A_7	$(8.29 \pm 1.73) \times 10^4$	Ea_7	69.2 ± 8.4
A_8	$(6.46 \pm 0.70) \times 10^3$	Ea_8	65.6 ± 33.4
A_9	$(2.86 \pm 0.44) \times 10^{11}$	Ea_9	135.7 ± 40.4
A_{10}	$(2.68 \pm 0.42) \times 10^9$	Ea_{10}	124.3 ± 18.7
A_{12}	$(2.58 \pm 0.71) \times 10^{12}$	Ea_{12}	147.1 ± 33.4
A_{13}	$(4.09 \pm 0.81) \times 10^1$	Ea_{13}	49.8 ± 10.4
A_{14}	$(2.08 \pm 1.98) \times 10^3$	Ea_{14}	124.1 ± 38.1
A_{16}	$(3.60 \pm 3.94) \times 10^3$	Ea_{16}	69.2 ± 43.9
A_{17}	$(5.10 \pm 4.81) \times 10^{-2}$	Ea_{17}	38.7 ± 27.0
A_{20}	$(5.46 \pm 1.51) \times 10^1$	Ea_{20}	69.9 ± 25.0

Crucial steps for the formation of molecular nitrogen are r_{10} and r_{14}, while the most important elementary reactions for the oxidation of the hydrocarbon are r_{10}, r_{12} and r_{14}. Obviously, r_{10} and r_{12} are important steps, since they are present in the consumption/production rates (Eqs. (18)–(21)). Both steps had high activation energies (around 124 and 147 kJ/mol respectively). Small variations on temperature are very likely to affect the reaction rate, since its dependence increases exponentially. This could be related with the activation of the hydrocarbon when the temperature barrier (around 350 °C) is surpassed boosting the hydrocarbon oxidation.

The formation of NO_2 depends on steps 5 (formation) and 16 (consumption). The formation exceeds the consumption of NO_2 at temperatures lower than 250 °C, switching the trend at temperatures above 250 °C, which explains very well the experimental findings.

Although the concentrations of NO_2 in the system during the experiments were relatively small compared to the concentrations of NO, its formation was observed and should be taken into account as the model predicts.

Then, the small contribution of the step 17, compared to the other elementary reactions, could easily be neglected. It seems that the formation of isocyanates is not as important as initially thought, even with the higher catalytic activity using hexadecane as a reducing agent instead of octane.

It is important to mention that only surface reactions were considered in this mechanism, whereas the gas-phase interactions were neglected. Because of the small dimensions in the microreactor and high surface-to-volume ratio, the occurrence of homogeneous gas-phase reactions is considerably reduced, leaving the heterogeneously catalyzed reactions as the only ones taking place.

One of the attractive features of the presented model is that it is valid in a large reactant concentrations region as well as over a large temperature range (150–550 °C). Most important, it helps to understand the SCR of NO_x with a second-generation biodiesel component, i.e., hexadecane.

SCR of NO_x with octane has been successfully performed in a microreactor and the obtained results were compared with conventional minireactors [9]. No previous kinetic studies of the SCR of NO with hexadecane have been presented. Kinetic experiments have been performed in a parallel study in a minireactor at our group [43]. When comparing reaction orders of hexadecane with respect to hexadecane, for the case of minireactors, the calculated orders varied from 0 at temperatures below 250 °C (when the partial oxidation of the hydrocarbon remains low) to 1.23 at 550 °C. For the microreactor case, the reaction orders were correspondingly increasing, reaching a maximum of 1.73 at 550 °C, and being zero at temperatures below 250 °C. The effect of hexadecane in the reaction rate appears to be stronger for the case of the microreactor at elevated temperatures (above 450 °C). At temperatures of 350–400 °C, reaction orders for the mini and microreactors were very similar, i.e., 0.54 and 0.62 (350 °C) and 1.06 and 0.98 (400 °C) respectively. For the reaction orders of NO in NO similarities were also found. In minireactors, reaction orders of NO in NO were in the range of 0.52–0.67 at the studied temperatures (250–550 °C). The values obtained in the microreactor were in the range of 0.49–0.71 for the same temperature range.

Interestingly, the experimental reaction rates (turnover frequencies) obtained in the microreactor exceeded those for the minireactor. The catalyst used for the kinetic experiments in the minireactor has been developed and optimized by our group [24]. This is not the case for the coating of the microchannels, where more research and catalytic characterization is still needed. In that

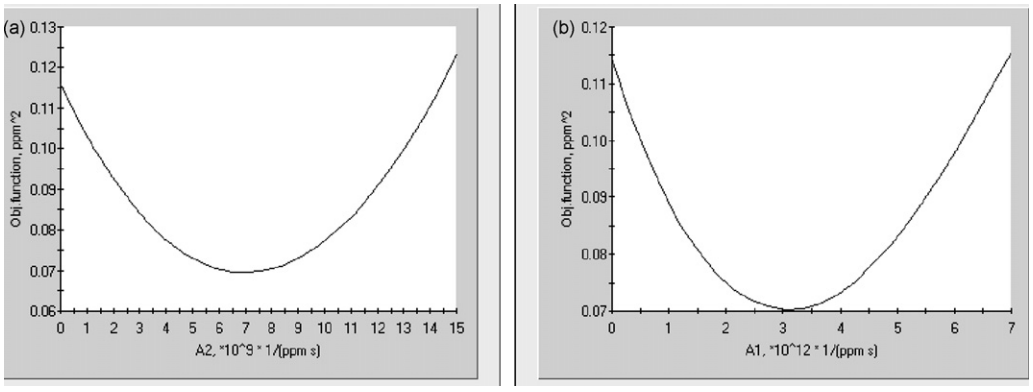

Fig. 9. Sensitivity plots for parameters A_2 (a) and A_{12} (b).

sense, obtaining higher reaction rates in this system (sometimes two orders of magnitude higher) shows the strong potential of these devices for kinetic experiments: not only the results are obtained faster, but better conversion of reactants per gram of catalyst could be achieved as well. Such advantage of microreactors over minireactors is important if the former are to be used as a standard equipment for kinetic measurements.

7. Conclusions

A gas-phase microreactor (∅ = 460 μm) coated with Ag/Al_2O_3 was used for the kinetic investigations of the hydrocarbon-assisted selective catalytic reduction of NO_x. As a model compound, hexadecane, a high quality diesel fuel and a representative component of the second-generation biodiesels, was employed. A kinetic model based on the experimental data was developed. The kinetic parameters were estimated with non-linear regression by using a plug flow model for the microchannels. The model assumes molecular adsorption of NO and CO and dissociative adsorption of O_2. After hexadecane is chemisorbed on the surface, its C–H bond is split by adsorbed oxygen. The oxidized hexadecane reacts with surface nitrates to form adsorbed R-CNO species that further on, via intermediates, reacts to yield N_2 and oxygenated hydrocarbons. The model described the experimental data fairly well.

The nature of the hydrocarbon was proved to influence the SCR of NO_x. At low temperatures, below 350 °C, the large size of the hexadecane molecule was suggested to inhibit the adsorption of nitrogen oxides on the surface, producing a detriment in the NO to N_2 activity. On the other hand, when the temperature was above 350 °C, the hexadecane was oxidized easier and positive effect of the increasing hydrocarbon concentration on the SCR activity was observed.

Although the degree of explanation of the model was very high (>95%), some high standard errors were also found. However, the generality of the model and its validity for a broad reactant concentrations and a wide temperature range (150–550 °C), make it a valuable tool for understanding the hexadecane-assisted SCR of NO_x.

Acknowledgements

Paul Ek at the Laboratory of Analytic Chemistry, Åbo Akademi University is gratefully acknowledged for the LA-ICP-MS analysis. The financial support from the Graduate School on Chemical Engineering for J.R. Hernández Carucci is also gratefully acknowledged. This work is part of the activities at the Åbo Akademi Process Chemistry Centre within the Finnish Centre of Excellence Programme (2006–2011) appointed by the Academy of Finland.

References

[1] M.A. Liauw, M. Baerns, R. Broucek, O.V. Buyevskaya, J.-M. Commenge, J.-P. Corriou, L. Falk, K. Gebauer, H.J. Hefter, O.-U. Langer, H. Lowe, M. Matlosz, A. Renken, A. Rouge, R. Schenk, N. Steinfeldt, St. Walter, Periodic operation in microchannel reactors. Microreaction technology: industrial prospects, in: Proceedings of the 3rd International Conference on Microreaction Technology, Frankfurt, Germany, 1999, pp. 224–234.
[2] K.F. Jensen, Microreaction engineering—is small better? Chem. Eng. Sci. 56 (2) (2001) 293–303.
[3] G. Kolb, V. Hessel, Micro-structured reactors for gas phase reactions, Chem. Eng. J. 98 (2004) 1–38.
[4] L. Kiwi-Minsker, A. Renken, Microstructured reactors for catalytic reactions, Catal. Today 110 (2005) 2–14.
[5] P.L. Mills, D.J. Quiram, J.F. Ryley, Microreactor technology and process miniaturization for catalytic reactions—a perspective on recent developments and emerging technologies, Chem. Eng. Sci. 62 (2007) 6992–7010.
[6] W. Ehrfeld, V. Hessel, H. Löwe, Microreactors—New Technology for Modern Chemistry, Wiley-VCH, Weinheim, 2000.
[7] J.-M. Commenge, L. Falk, J.-P. Corriu, M. Matlosz, Analysis of microstructured reactor characteristics for process miniaturization and intensification, Chem. Eng. Technol. 28 (2005) 446–458.
[8] G. Veser, Experimental and theoretical investigation of H_2 oxidation in a high-temperature catalytic microreactor, Chem. Eng. Sci. 56 (2001) 1265–1273.
[9] J.R. Hernández Carucci, K. Arve, K. Eränen, D.Yu. Murzin, T. Salmi, Microreactors for environmental catalysis—selective catalytic reduction of NO_x with hydrocarbons over a Ag/alumina catalyst, Catal. Today 133–135 (2008) 448–454.
[10] K. Shimizu, A. Satsuma, Hydrogen assisted urea-SCR and NH3-SCR with silver-alumina as highly active and SO2-tolerant de-NOx catalysis, Appl. Catal. B 77 (2007) 202–205.
[11] M.H. Kim, I.-S. Nam, New opportunity for HC-SCR technology to control NO_x emission from advanced internal combustion engines, Catalysis 18 (2005) 116–185.
[12] M. Iwamoto, H. Yahiro, S. Shundo, Y. Yu-u, N. Mizuno, Influence of sulfur dioxide on catalytic removal of nitric oxide over copper ion-exchanged ZSM-5 zeolite, Appl. Catal. 69 (1991) L15–L19.
[13] W. Held, A. König, T. Ritcher, L. Puppe, Catalytic NOx reduction in net oxidizing exhaust gas. SAE Paper No. 900496, 1990.
[14] R. Burch, P.J. Millington, Selective reduction of NOx by hydrocarbons in excess oxygen by alumina- and silica-supported catalysts, Catal. Today 29 (1996) 37–42.
[15] K. Miyadera, Alumina-supported silver catalysts for the selective reduction of nitric oxide with propene and oxygen-containing organic compounds, Appl. Catal. B 2 (1993) 199–205.
[16] K.A. Bethke, H.H. Kung, Supported Ag catalysts for the lean reduction of NO with C_3H_6, J. Catal. 172 (1997) 93–102.
[17] A. Martinez-Arias, M. Fernandez-Garcia, A. Iglesias-Juez, J.A. Anderson, J.C. Conesa, J. Soria, Study of the lean NOx reduction with C_3H_6 in the presence of water over silver/alumina catalysts prepared from inverse microemulsions, Appl. Catal. B 28 (2000) 29–41.
[18] A. Fritz, V. Pitchon, The current state of research on automotive lean NOx catalysis, Appl. Catal. B 13 (1997) 1–25.
[19] K. Shimizu, J. Shibata, H. Yoshida, A. Satsuma, T. Hattori, Silver-alumina catalysts for selective reduction of NO by higher hydrocarbons: structure of active sites and reaction mechanism, Appl. Catal. B 30 (2001) 151–162.
[20] K. Sato, T. Yoshinari, Y. Kintaichi, M. Haneda, H. Hamada, Remarkable promoting effect of rhodium on the catalytic performance of Ag/Al_2O_3 for the selective reduction of NO with decane, Appl. Catal. B 44 (2003) 67–78.
[21] S. Satokawa, J. Shibata, K.-I. Shimizu, A. Satsuma, T. Hattori, Promotion effect of H_2 on the low temperature activity of the selective reduction of NO by light hydrocarbons over Ag/Al_2O_3, Appl. Catal. B 42 (2003) 179–186.
[22] A. Satsuma, K.-I. Shimizu, In situ FT/IR study of selective catalytic reduction of NO over alumina-based catalysts, Prog. Energy Combust. Sci. 29 (2003) 71–84.
[23] K. Eränen, L.-E. Lindfors, F. Klingstedt, D.Yu. Murzin, Continuous reduction of NO with octane over a silver/alumina catalyst in oxygen-rich exhaust gases: combined heterogeneous and surface-mediated homogeneous reactions, J. Catal. 219 (2003) 25–40.
[24] K. Arve, L. Čapek, F. Klingstedt, K. Eränen, L.-E. Lindfors, D.Yu. Murzin, J. Dědeček, Z. Sobalik, B. Wichterlová, Preparation and characterisation of Ag/alumina catalysts for the removal of NOx emissions under oxygen rich conditions, Top. Catal. 30/31 (2004) 91–95.
[25] F. Klingstedt, K. Eränen, L.-E. Lindfors, S. Andersson, L. Cider, C. Landberg, E. Jobson, L. Eriksson, T. Ilkenhans, D. Webster, A highly active Ag/alumina catalytic converter for continuous HC-SCR during lean-burn conditions: from laboratory to full-scale vehicle tests, Top. Catal. 30/31 (2004) 27–30.
[26] K. Eränen, F. Klingstedt, K. Arve, L.-E. Lindfors, D.Yu. Murzin, On the mechanism of the selective catalytic reduction of NO with higher hydrocarbons over a silver/alumina catalyst, J. Catal. 227 (2004) 328–343.
[27] R. Burch, J.P. Breen, F.C. Meunier, A review of the selective reduction of NOx with hydrocarbons under lean-burn conditions with non-zeolitic oxide and platinum group metal catalysts, Appl. Catal. B 39 (2002) 283–303.
[28] E.F. Iliopoulou, A.P. Evdou, A.A. Lemonidou, I.A. Vasalos, Ag/alumina catalysts for the selective catalytic reduction of NOx using various reductants, Appl. Catal. A 274 (2004) 179–189.
[29] G.E. Marnellos, E.A. Efthimiadis, I.A. Vasalos, Mechanistic and kinetic analysis of the NO_x selective catalytic reduction by hydrocarbons in excess O_2 over In/Al_2O_3 in the presence of SO_2 and H_2O, Appl. Catal. B 48 (2004) 1–15.
[30] F.C. Meunier, V. Zuzaniuk, J.P. Breen, M. Olsson, J.R.H. Ross, Mechanistic differences in the selective reduction of NO by propene over cobalt- and silver-promoted alumina catalysts: kinetic and in situ DRIFTS study, Catal. Today 59 (2000) 287–304.
[31] K. Arve, H. Backman, F. Klingstedt, K. Eränen, D.Yu. Murzin, Kinetic considerations of H_2 assisted hydrocarbon selective catalytic reduction of NO over Ag/Al_2O_3. I. Kinetic behaviour, Appl. Catal. A 303 (2006) 96–102.
[32] H. Backman, K. Arve, F. Klingstedt, D.Yu. Murzin, Kinetic considerations of H2 assisted hydrocarbon selective catalytic reduction of NO over Ag/Al2O3. II. Kinetic modelling, Appl. Catal. A (304) (2006) 86–92.
[33] J.P. Breen, R. Burch, C. Hardacre, C.J. Hill, C. Rioche, A fast transient kinetic study of the effect of H_2 on the selective catalytic reduction of NOx with octane using isotopically labelled ^{15}NO, J. Catal. 246 (2007) 1–9.
[34] D.Yu. Murzin, I. Kubickova, M. Snåre, P. Mäki-Arvela, Method for manufacture of hydrocarbons, European patent 05075068.6, 2005.
[35] I. Kubičková, M. Snåre, K. Eränen, P.-M. Arvela, D.Yu. Murzin, Hydrocarbons for diesel fuel via decarboxylation of vegetable oils, Catal. Today 106 (2005) 197–200.

[36] J.F. Moulder, W.F. Stickle, P.E. Sobol, K.D. Bomben, Handbook of X-ray Photoelectron Spectroscopy, Perkin Elmer Corp., Physical Electronics Division, USA, 1992.
[37] E. Seker, J. Cavataio, E. Gulari, P. Lorpongpaiboon, S. Osuwan, Nitric oxide reduction by propene over silver/alumina and silver-gold/alumina catalysts: effect of preparation methods, Appl. Catal. A 183 (1999) 121–134.
[38] K. Luo, X. Lai, C.-W. Yi, K.A. Davis, K.K. Gath, D.W. Goodman, The growth of silver on an ordered alumina surface, J. Phys. Chem. B 109 (2005) 4064–4068.
[39] R. Zapf, C. Becker-Willinger, K. Berresheim, H. Bolz, H. Gnaser, V. Hessel, G. Kolb, P. Loëb, A.-K. Pannwitt, A. Ziogas, Detailed characterization of various porous alumina-based catalyst coatings within microchannels and their testing for methanol steam reforming, Trans IChemE 81 (2003) 721–729.
[40] S.M. Wetterer, D.J. Lavrich, T. Cummings, S.L. Bernasek, G. Scoles, Energetics and kinetics of the physisorption of hydrocarbons on Au(111), J. Phys. Chem. B 102 (1998) 9266–9275.
[41] Y. Morikawa, H. Ishii, K. Seki, Theoretical study of n-alkane adsorption on metal surfaces, Phys. Rev. B 69 (2004) 041403/1–041403/4.
[42] K. Shimizu, J. Shibata, A. Satsuma, Kinetic and in situ infrared studies on SCR of NO with propane by silver–alumina catalyst: role of H_2 on O_2 activation and retardation of nitrate poisoning, J. Catal. 239 (2006) 402–409.
[43] K. Arve, J.R. Hernández Carucci, K. Eränen, A. Aho, D. Yu. Murzin, Kinetic behaviour of HC-SCR over Ag/alumina catalyst using a model paraffinic second generation bio-diesel compound, submitted for publication.
[44] T. Miyadera, K. Yoshida, Alumina-supported catalysts for the selective reduction of nitric oxide by propene, Chem. Lett. (1993) 1483–1486.
[45] P. Sazama, L. Čapek, H. Drobná, Z. Sobalík, J. Dědeček, K. Arve, B. Wichterlová, Enhancement of decane-SCR-NOx over Ag/alumina by hydrogen. Reaction kinetics and in situ FTIR and UV–vis study, J. Catal. 232 (2005) 302–317.
[46] K. Arve, F. Klingstedt, K. Eränen, J. Wärnå, L.-E. Lindfors, D.Yu. Murzin, Kinetics of NOx reduction over Ag/alumina by higher hydrocarbon in excess of oxygen, Chem. Eng. J. 107 (2005) 215–220.
[47] K. Arve, H. Backman, F. Klingstedt, K. Eränen, D.Yu. Murzin, Hydrogen as a remedy for the detrimental effect of aromatic and cyclic compounds on the HC-SCR over Ag/alumina, Appl. Catal. B 70 (2007) 65–72.
[48] V. Houel, P. Millington, R. Rajaram, A. Tsolakis, Fuel effects on the activity of silver hydrocarbon-SCR catalysts, Appl. Catal. B 73 (2007) 203–207.
[49] R. Burch, Knowledge and know-how in emission control for mobile applications, Cat. Rev.–Sci. Eng. 46 (2004) 271–333.
[50] P. Konova, K. Arve, F. Klingstedt, P. Nikolov, A. Naydenov, N. Kumar, D.Yu. Murzin, A combination of Ag/alumina and Ag modified ZSM-5 to remove NOx and CO during lean conditions, Appl. Catal. B 70 (2007) 138–145.
[51] K.J. Laidler, Chemical Kinetics, 3rd ed., Harper and Row Publishers, New York, 1987.
[52] P. Denton, Y. Schuurman, A. Giroir-Fendler, H. Praliaud, M. Primet, C. Mirodatos, N_2O as an intermediate for the formation of N_2 during SCR (NO): stationary and transient conditions, C.R. Acad. Sci., Ser. IIc: Chim. 3 (2000) 437–441.
[53] M.I. Temkin, The kinetics of some industrial heterogeneous catalytic reactions, Adv. Catal. 28 (1979) 173–291.
[54] D.Yu. Murzin, T. Salmi, Catalytic Kinetics, Elsevier, Amsterdam, 2005.
[55] H. Haario, ModEst 6. 0—A User's Guide, ProfMath, Helsinki, 2001.